


# Functional Characterization of 40 CYP3A4 Variants by Assessing Midazolam 1'-Hydroxylation and Testosterone 6 $\beta$ -Hydroxylation<sup>§</sup>

Masaki Kumondai, Evelyn Marie Gutiérrez Rico, Eiji Hishinuma, Akiko Ueda, Sakae Saito, Daisuke Saigusa, Shu Tadaka, Kengo Kinoshita, Tomoki Nakayoshi, Akifumi Oda, Ai Abe, Masamitsu Maekawa, Nariyasu Mano, Noriyasu Hirasawa, and  Masahiro Hiratsuka

Laboratory of Pharmacotherapy of Life-Style Related Diseases, Graduate School of Pharmaceutical Sciences (M.K., E.M.G.R., N.H., M.H.), Tohoku Medical Megabank Organization (E.H., S.S., D.S., S.T., K.K., M.H.), Advanced Research Center for Innovations in Next-Generation Medicine (E.H., A.U., N.H., M.H.), and Laboratory of Clinical Pharmacy, Faculty of Pharmaceutical Sciences (A.A., M.M., N.M.), Tohoku University, Sendai, Japan; Faculty of Pharmacy, Meijo University, Nagoya, Japan (T.N., A.O.); and Department of Pharmaceutical Sciences, Tohoku University Hospital, Sendai, Japan (M.M., N.M., N.H., M.H.)

Received September 28, 2020; accepted December 24, 2020

## ABSTRACT

CYP3A4 is among the most abundant liver and intestinal drug-metabolizing cytochrome P450 enzymes, contributing to the metabolism of more than 30% of clinically used drugs. Therefore, interindividual variability in CYP3A4 activity is a frequent cause of reduced drug efficacy and adverse effects. In this study, we characterized wild-type CYP3A4 and 40 CYP3A4 variants, including 11 new variants, detected among 4773 Japanese individuals by assessing CYP3A4 enzymatic activities for two representative substrates (midazolam and testosterone). The reduced carbon monoxide–difference spectra of wild-type CYP3A4 and 31 CYP3A4 variants produced with our established mammalian cell expression system were determined by measuring the increase in maximum absorption at 450 nm after carbon monoxide treatment. The kinetic parameters of midazolam and testosterone hydroxylation by wild-type CYP3A4 and 29 CYP3A4 variants ( $K_m$ ,  $k_{cat}$ , and catalytic efficiency) were determined, and the causes of their kinetic

differences were evaluated by three-dimensional structural modeling. Our findings offer insight into the mechanism underlying interindividual differences in CYP3A4-dependent drug metabolism. Moreover, our results provide guidance for improving drug administration protocols by considering the information on CYP3A4 genetic polymorphisms.

## SIGNIFICANCE STATEMENT

CYP3A4 metabolizes more than 30% of clinically used drugs. Interindividual differences in drug efficacy and adverse-effect rates have been linked to ethnicity-specific differences in CYP3A4 gene variants in Asian populations, including Japanese individuals, indicating the presence of CYP3A4 polymorphisms resulting in the increased expression of loss-of-function variants. This study detected alterations in CYP3A4 activity due to amino acid substitutions by assessing the enzymatic activities of coding variants for two representative CYP3A4 substrates.

## Introduction

CYP3A4 is the most abundant liver and intestinal drug-metabolizing cytochrome P450 enzyme, contributing to the metabolism of more than

M.H. was supported by grants from Japan Agency for Medical Research and Development (AMED) [Grant 20kk0305009], Takahashi Industrial and Economic Research Foundation, and Smoking Research Foundation. M.K. was supported by Japan Society for the Promotion of Science [Grant 19J10744] and the Pharmaceutical Society of Japan [Grant N-170603]. S.S., K.K., S.T., and D.S. were supported by grants from AMED [Grant JP20km0105001 and JP20km0105002]. This research was also supported in part by the Tohoku Medical Megabank Project: Promoting Public Utilization of Advanced Research Infrastructure, and the Sharing and Administrative Network for Research Equipment funded by the Ministry of Education, Culture, Sports, Science and Technology (MEXT). K.K. and S.T. were supported by grants for the Facilitation of R&D Platform for AMED Genome Medicine Support from AMED (Grant Number JP20km0405001).

The authors declare no conflict of interest.

<https://doi.org/10.1124/dmd.120.000261>.

<sup>§</sup>This article has supplemental material available at [dmd.aspetjournals.org](http://dmd.aspetjournals.org).

30% of medications (Zanger and Schwab, 2013; Jackson et al., 2018; Niwa et al., 2020). Interindividual variability in CYP3A4 activity and expression influences drug responsiveness, efficacy, and adverse-effect rates (Lamba et al., 2002a). Besides the various factors that contribute to this variability, including CYP3A4 inducers and inhibitors and food-drug and drug-drug interactions, CYP3A4 genetic variations also affect drug responses (Racha et al., 2003; Huang et al., 2008; Elens et al., 2013; Hendriks et al., 2020). CYP3A5 genetic polymorphisms, including CYP3A5\*3, have been widely investigated because of their high allele frequencies and clinical impact on the variability of CYP3A activity. CYP3A4 gene variations may be overlooked because of the higher impact of some CYP3A5 variants on activity. However, CYP3A4 gene variations should also be investigated to elucidate their influence on the combinational effects of CYP3A4 and CYP3A5 enzymatic activity and CYP3A in vivo activity (Fukushima-Uesaka et al., 2004; Lee et al., 2005; Zhou et al., 2017). For instance, several CYP3A4 variant alleles, including CYP3A4\*1B (a promoter variant) and \*22 (an intronic variant), reduce mRNA levels or cause splicing defects, although

**ABBREVIATIONS:** CO, carbon monoxide; CPR, cytochrome P450 oxidoreductase; 3D, three-dimensional; LC-MS/MS, liquid chromatography-tandem mass spectrometry; m/z, mass-to-charge ratio; PCR, polymerase chain reaction; SNV, single nucleotide variation; SRS, substrate recognition site; WGS, whole-genome sequencing.

*CYP3A4*\*6, \*17, \*20, and \*26 are associated with diminished enzymatic activities by loss of function (Lamba et al., 2002a; Elens et al., 2013; Werk et al., 2014). The identification of these variants can improve patient safety and treatment efficacy; thus, increased dose-adjusted tacrolimus concentration levels are achieved in transplant patients carrying a loss-of-function genotype (*CYP3A4*\*20) (Gómez-Bravo et al., 2018). Hence, *CYP3A4* genotyping improves predictive outcomes.

The Human Cytochrome P450 Allele Nomenclature Database [https://www.pharmvar.org/gene/CYP3A4 (accessed September 21st, 2020)] contains records of *CYP3A4* genetic polymorphisms (*CYP3A4*\*2–\*24, *CYP3A4*\*26, and *CYP3A4*\*28–\*34). Moreover, several whole-genome sequencing (WGS) studies have identified *CYP3A4* genetic variations, including c.1165C>T (Pro389Ser) and c.1423C>G (Leu475Val) (Apellaniz-Ruiz et al., 2015). A WGS project of the Tohoku Medical Megabank Organization, which targeted 4773 Japanese individuals, identified numerous genetic variations, including single nucleotide variations (SNVs), as shown in Table 1 [https://jmorp.megabank.tohoku.ac.jp (accessed August 30th, 2020)]. The identification of rare genetic variants, which may cause interindividual differences in drug efficacy and adverse reactions, facilitates the development of personalized medicine (Fujikura et al., 2015; Schärfe et al., 2017). *CYP3A4* rare genetic variants have been implicated in high-dose simvastatin-related myopathy and affect serum voriconazole concentrations linked to adverse drug reactions (Ingelman-Sundberg et al., 2018). Although the *CYP3A4* SNVs analyzed in this study are relatively rare (Table 1), their effects on CYP3A4 activity should be determined to improve treatment outcomes and manage adverse effects.

Heterologous expression systems can be employed to evaluate the effects of *CYP3A4* polymorphisms in vitro and complement in vivo analysis data. Performing in vivo assays is challenging because of low allele frequencies and increased patient burden. However, all CYP3A4 variant proteins should be evaluated using the same protocol and experimental conditions because methodological differences between studies may lead to inconsistent kinetic parameters for some variants (Hiratsuka, 2012). To date, characterization studies have used cDNA-based heterologous expression systems, including *Escherichia coli*, baculoviruses, and mammalian cell systems (Eiselt et al., 2001; Lee et al., 2005; Maekawa et al., 2010; Kumondai et al., 2018; Saito et al., 2018; Watanabe et al., 2018; Gutiérrez Rico et al., 2020). However, accurate assessments are limited by interspecies differences of post-translational modifications. Thus, mammalian cell expression systems should be preferred to evaluate the function of human CYP3A4 variants in drug metabolism (Clark and Pazdernik, 2016). Recently, an intronic *CYP2D6* mutation was evaluated using a minigene expression system with transfected whole *CYP2D6* sequences (<5 kb) (Zanger et al., 2020). Minigenes may aid the assessment of CYP3A4 levels. However, genomic DNA expression using minigenes, including the whole *CYP3A4* gene (>20 kb), is challenging because transfection efficiency decreases with increased DNA length (Hornstein et al., 2016). Therefore, we used our heterologous expression system consisting of 293FT cells coexpressing CYP3A4, cytochrome P450 oxidoreductase (CPR), and cytochrome b<sub>5</sub> (Kumondai et al., 2020).

Here, we functionally characterized wild-type CYP3A4 (*CYP3A4.1*) and 40 CYP3A4 allelic variants, including 11 novel variants identified in 4773 Japanese individuals, by using two representative CYP3A4 substrates (midazolam and testosterone). Notably, clinical and in vitro studies have assessed the functional differences and drug-drug interactions related to CYP3A4, including cytochrome P450 variants with substrate-specific enzymatic activities (Foti et al., 2010; Hiratsuka, 2016; Xiao et al., 2019). Moreover, carbon monoxide (CO)-difference spectroscopy and three-dimensional (3D) structure analysis were

TABLE 1  
CYP3A4 allelic variants characterized in this study

Variants	Protein	Nucleotide Mutations	Amino Acid Substitutions
<i>CYP3A4</i> *1	CYP3A4.1		Ser222Pro
<i>CYP3A4</i> *2	CYP3A4.2	664T>C	Met445Thr
<i>CYP3A4</i> *3	CYP3A4.3	1334T>C	Ile118Val
<i>CYP3A4</i> *4	CYP3A4.4	352A>G	Pro218Arg
<i>CYP3A4</i> *5	CYP3A4.5	653C>G	Gly56Asp
<i>CYP3A4</i> *7	CYP3A4.7	167G>A	Arg130Gln
<i>CYP3A4</i> *8	CYP3A4.8	389G>A	Val170Ile
<i>CYP3A4</i> *9	CYP3A4.9	508G>A	Asp174His
<i>CYP3A4</i> *10	CYP3A4.10	520G>C	Thr363Met
<i>CYP3A4</i> *11	CYP3A4.11	1088C>T	Leu373Phe
<i>CYP3A4</i> *12	CYP3A4.12	1117C>T	Pro416Leu
<i>CYP3A4</i> *13	CYP3A4.13	1247C>T	Leu15Pro
<i>CYP3A4</i> *14	CYP3A4.14	44T>C	Arg162Gln
<i>CYP3A4</i> *15	CYP3A4.15	485G>A	Thr185Ser
<i>CYP3A4</i> *16	CYP3A4.16	554C>G	Phe189Ser
<i>CYP3A4</i> *17	CYP3A4.17	566T>C	Leu293Pro
<i>CYP3A4</i> *18	CYP3A4.18	878T>C	Pro467Ser
<i>CYP3A4</i> *19	CYP3A4.19	1399C>T	488Frameshift
<i>CYP3A4</i> *20		1461_1462insA	Tyr319Cys
<i>CYP3A4</i> *21	CYP3A4.21	956A>G	Arg162Trp
<i>CYP3A4</i> *23	CYP3A4.23	484C>T	Gln200His
<i>CYP3A4</i> *24	CYP3A4.24	600A>T	Pro389Ser
		1165C>T	Leu475Val
		1423C>G	Leu22Phe
<i>CYP3A4</i> *28	CYP3A4.28	64C>G	Phe113Ile
<i>CYP3A4</i> *29	CYP3A4.29	337T>A	His324Gln
<i>CYP3A4</i> *31	CYP3A4.31	972C>A	Ile335Thr
<i>CYP3A4</i> *32	CYP3A4.32	1004T>C	Ala370Ser
<i>CYP3A4</i> *33	CYP3A4.33	1108G>T	Ile427Val
<i>CYP3A4</i> *34	CYP3A4.34	1279A>G	Thr138Ala
	Novel variant 1	412A>G	Met256Ile
	Novel variant 2	768G>C	Ile300Val
	Novel variant 3	898A>G	Thr323Ala
	Novel variant 4	967A>G	Met353Leu
	Novel variant 5	1057A>T	Ile369Val
	Novel variant 6	1105A>G	Ile369Asn
	Novel variant 7	1106T>A	Ala370Val
	Novel variant 8	1109C>T	Arg372Thr
	Novel variant 9	1115G>C	Tyr399Ser
	Novel variant 10	1196A>C	Ala448Ser
	Novel variant 11	1342G>T	

performed to gain insights into functional alterations caused by CYP3A4 variants.

## Materials and Methods

**Chemicals.** The following reagents were purchased from commercial sources: midazolam [PubChem Compound ID (CID) 4192] and flunitrazepam (Wako Pure Chemical Industries, Osaka, Japan), 1'-hydroxymidazolam (CID 107917) and 6β-hydroxytestosterone-d7 (Corning Incorporated, NY), testosterone (CID 6013) and 6β-testosterone (CID 65543) (Sigma-Aldrich, Steinheim, Germany), NADH and NADPH (Oriental Yeast, Tokyo, Japan), polyclonal anti-human CYP3A4 antibody (ab3572) (Abcam, Cambridge, UK), horseradish peroxidase-conjugated goat anti-rabbit IgG (ProteinSimple, Tokyo, Japan), dimanganese decacarbonyl (Sigma-Aldrich), and sodium cyanide and cytochrome c from horse heart (Nacalai Tesque, Kyoto, Japan). All other chemicals and reagents were of the highest quality commercially available.

**Detection of CYP3A4 Sequence Alterations by Sanger Sequencing Analysis.** PCR amplification was conducted using peripheral blood leukocyte genome DNA isolated from whole blood using the Gentra Puregene Blood Kit (Qiagen, Hilden, Germany), as described previously (Nagasaki et al., 2015). Whole blood samples were obtained from Japanese subjects participating in the community-based cohort study conducted by the Tohoku Medical Megabank Organization, and written informed consent was obtained from all subjects before sample collection. Primers were used to amplify sequences containing each *CYP3A4* exon (Supplemental Table 1). PCR amplification was performed with genomic DNA samples (10 ng), 2× AmpliTaq Gold 360 Master Mix (Applied

Biosystems, Foster City, CA), and 0.5  $\mu\text{M}$  of each primer in a total volume of 20  $\mu\text{l}$ . Thermal cycling conditions included an initial denaturation step at 95°C for 10 minutes, followed by 30 cycles of denaturation at 95°C for 30 seconds, annealing at 60°C for 30 seconds, extension at 72°C for 30 seconds (for exons 2–12) or 1 minute (for exons 1 and 13), and a final extension at 72°C for 7 minutes. The PCR products were purified using columns and analyzed by Sanger sequencing utilizing the same primers for each exon as in the PCR except for the forward sequencing reaction of exon 1 (5'-CAGGCGTGGAAACACAATGGTGG-3') and reverse sequencing reaction of exon 11 (5'-TGTGGATGACTGTAGTTTC-3'). To determine the linkage between two SNVs identified in one subject, the respective PCR fragments were ligated into the pcDNA3.4 vector (ThermoFisher Scientific), and the ligation products were transformed into *E. coli*. Single colonies of the transformants were collected, and the plasmids were isolated and analyzed by Sanger sequencing. This analysis was performed in accordance with the Declaration of Helsinki, and prior written informed consent was obtained from all participants.

**Construction of CYP3A4 cDNA Expression Vectors.** The wild-type CYP3A4 (*CYP3A4\**) plasmid used in this study has been described in a previous report (Sakurai et al., 2005). A plasmid containing *CYP3A4\**1 cDNA was used as a template to generate *CYP3A4* allelic variant constructs (*CYP3A4\**2–*CYP3A4\**5, *CYP3A4\**7–*CYP3A4\**21, *CYP3A4\**23, *CYP3A4\**24, Pro389Ser, Leu475Val, *CYP3A4\**28, *CYP3A4\**29, *CYP3A4\**31–*CYP3A4\**34, Thr138Ala, Met256Ile, Ile300Val, Thr323Ala, Met353Leu, Ile369Val, Ile369Asn, Ala370Val, Arg372Thr, Tyr399Ser, and Ala448Ser) using primer sets described in Supplemental Table 2 with the QuikChange Site-Directed Mutagenesis Kit (Stratagene, La Jolla, CA) following the manufacturer's instructions. All prepared constructs were confirmed by Sanger sequencing. Wild-type and variant *CYP3A4* cDNAs were subcloned into the mammalian expression vector pcDNA3.4. A mock plasmid, including the pcDNA3.4 vector, was prepared as previously reported (Kumondai et al., 2018; Saito et al., 2018).

**Expression of CYP3A4 Variants in 293FT Cells.** The 293FT cells (ThermoFisher Scientific) were cultured in Dulbecco's modified Eagle's medium (Nacalai Tesque) containing 10% fetal bovine serum at 37°C under 5% CO<sub>2</sub>. Cells were plated at a density of  $2.2 \times 10^6$  cells per 100-mm dish; 24 hours after plating, the cells were transfected with a plasmid carrying CYP3A4 (9.6  $\mu\text{g}$ ), CPR (0.2  $\mu\text{g}$ ), and cytochrome b<sub>5</sub> (0.2  $\mu\text{g}$ ) cDNA using 30  $\mu\text{l}$  of 1.0 mg/ml of Polyethylenimine Max (Polysciences, Inc., Warrington, PA), according to previously described methods (Kumondai et al., 2020). After incubation for 12 hours at 37°C, 0.25 mM of 5-aminolevulinic acid hydrochloride (Nacalai Tesque) and 0.25 mM iron (II) sulfate heptahydrate (Wako) were added to the medium. After incubation for 48 hours post-transfection at 37°C, the cells were scraped from the plates, and the microsomal fractions were prepared as previously described (Kumondai et al., 2020). Protein concentrations were determined using the BCA Protein Assay Kit (ThermoFisher Scientific).

**Western Blotting.** CYP3A4 levels were quantified with an immunoassay using the Wes system (ProteinSimple). Each well was loaded with 25  $\mu\text{g}/\text{ml}$  microsomes. CYP3A4 was detected using a polyclonal anti-human CYP3A4 antibody (diluted 1:100) and horseradish peroxidase-conjugated goat anti-rabbit IgG. A total protein assay was performed to normalize each signal using 25  $\mu\text{g}/\text{ml}$  microsomes following the manufacturer's instructions. Recombinant human CYP3A4 Supersomes (Coming Incorporated) were used as the standard to quantify the CYP3A4 protein level.

**CO-Difference Spectroscopy.** The cytochrome P450 holoprotein content was spectrophotometrically measured according to a previously reported method based on the established protocol by Omura and Sato (Kumondai et al., 2020).

**Measurement of NADPH-Cytochrome c Reduction Activity and Microsomal Cytochrome b<sub>5</sub> Content Determination.** The activity of CPR and the content of cytochrome b<sub>5</sub> were spectrophotometrically evaluated as previously described (Kumondai et al., 2020).

**Midazolam 1'-Hydroxylation.** CYP3A4 midazolam 1'-hydroxylation activity was determined using a previously described method with several modifications (El Mahjoub and Staub, 2000). The reaction mixture, a total volume of 100  $\mu\text{l}$ , contained the following components: the microsomal fraction (50  $\mu\text{g}$ ), midazolam (1, 2, 4, 6, 8, 10, and 15  $\mu\text{M}$ ), and 100 mM potassium phosphate buffer (pH 7.4). After preincubation at 37°C for 3 minutes, reactions were initiated by adding 10 mM NADPH, and incubation continued at 37°C for 10 minutes. Reactions were terminated by adding 100  $\mu\text{l}$  of acetonitrile containing 500 nM flunitrazepam as an internal standard. After protein removal by centrifugation at 15,400g for

10 minutes, the supernatant was injected into a liquid chromatography-tandem mass spectrometry (LC-MS/MS) system, as previously described (Kumondai et al., 2020).

**Testosterone 6 $\beta$ -Hydroxylation Assay.** CYP3A4 testosterone 6 $\beta$ -hydroxylation activity was determined using a previously described method with several modifications (Nguyen et al., 2020). The reaction mixture, in a total volume of 100  $\mu\text{l}$ , contained the following components: the microsomal fraction (50  $\mu\text{g}$ ), testosterone (5, 10, 20, 50, 100, 200, or 500  $\mu\text{M}$ ), and 100 mM potassium phosphate buffer (pH 7.4). After preincubation at 37°C for 3 minutes, reactions were initiated by adding 10 mM NADPH, and the incubation was continued at 37°C for 10 minutes. The reactions were terminated by adding 100  $\mu\text{l}$  of acetonitrile containing 10  $\mu\text{M}$  6 $\beta$ -hydroxytestosterone-d7 as an internal standard. After protein removal by centrifugation at 15,400g for 10 minutes, the supernatant was injected into an LC-MS/MS system.

The 6 $\beta$ -hydroxytestosterone content was measured using the LC-MS/MS system in the positive ion detection mode at the electrospray ionization interface (QTRAP 6500 LC-MS/MS system; AB Sciex, MA). Separation by ultra-high-performance liquid chromatography was conducted using the Nexera Ultra-High-Performance Liquid Chromatography system (Shimadzu, Kyoto, Japan). Chromatographic separation was performed with a Kinetex C18 column (2.1  $\times$  50 mm, 5- $\mu\text{g}$  particle size; Phenomenex, Shimadzu) maintained at 40°C. Mobile phases were prepared with deionized water containing 0.1% formic acid as eluent A and acetonitrile containing 0.1% formic acid as eluent B. The flow rate was 300  $\mu\text{l}/\text{min}$ . The gradient program was as follows: elution was initiated with 10% B, followed by a linear gradient to 60% B from 1 to 7 minutes, held at 100% B for 2 minutes, and then immediately returned to the initial conditions, which were maintained for 3 minutes until the end of the run. Quantification analyses using Analyst Software (Sciex) were performed in the selected reaction monitoring mode in which ion transitions from the precursor into a product ion were monitored: mass-to-charge ratio ( $m/z$ ) 289.1 $\rightarrow$ 97.0 for testosterone (collision energy, 14 V),  $m/z$  305.0 $\rightarrow$ 269.1 for 6 $\beta$ -hydroxytestosterone (collision energy, 12 V), and  $m/z$  312.1 $\rightarrow$ 276.1 for 6 $\beta$ -hydroxytestosterone-d6 (collision energy, 4 V). The optimized mass spectrometry settings were as follows: entrance potential, 2.0 V; curtain gas, 25.0 psi; ion transfer voltage, 5500.0 V; temperature, 750.0°C; gas 1, 70.0 psi; gas 2, 30.0 psi; and collision gas, 12.0. Standard curves for 6 $\beta$ -hydroxytestosterone were constructed within the range of 100–30,000 nM using metabolite standards, with a quantification limit of 100 nM.

**Data Analysis.** Kinetic data, including the Michaelis constant ( $K_m$ ), turnover number ( $k_{cat}$ ), and catalytic efficiency ( $k_{cat}/K_m$ ) values, were determined using the Enzyme Kinetics Module of SigmaPlot 12.5 (Systat Software, Inc., Chicago, IL), a curve-fitting program based on nonlinear regression analysis. The normality of our data sets was initially assessed using the Shapiro-Wilk test. Statistical analyses for multiple comparisons were performed through variance analysis by Dunnett's T3 test or the Kruskal-Wallis method (IBM SPSS Statistics version 22; International Business Machines, Armonk, NY). All values are expressed as the means  $\pm$  S.D. of experiments performed in triplicate. Differences with  $P < 0.05$  were considered statistically significant. All assays and samples were prepared in triplicate to permit statistical analysis.

**3D Structural Modeling of CYP3A4.** The 3D structural modeling of CYP3A4 was based on the CYP3A4 X-ray structure of Sevrioukova and Poulos (2017) (Protein Data Bank code 5te8). Swiss-model was used to complement a part of the lacking structure in CYP3A4. After removing the substrate, midazolam or testosterone was docked with the CYP3A4 X-ray structure according to the CDOCKER protocol of Discovery Studio 2.5 (BIOVIA, CA). Docking iterations were conducted, taking into consideration the binding orientation and binding energies under the condition that the volume of the space was defined as 9, and the heme iron charge status was Fe<sup>3+</sup>. After replacing each substitution, structural optimization was conducted as previously described (Oda et al., 2005).

## Results

We performed resequencing for the subjects carrying novel SNVs, except for a subject carrying c.1342G>T because this DNA sample was not available for further sequencing. For SNVs located within exons, WGS identified 10 novel variants; these findings were identical with the results obtained using Sanger sequencing. Two SNVs (c.389G>A and c.412A>G) carried by one subject were located in different alleles (Supplemental Fig. 1). Thus, 11 novel CYP3A4 variants, including the

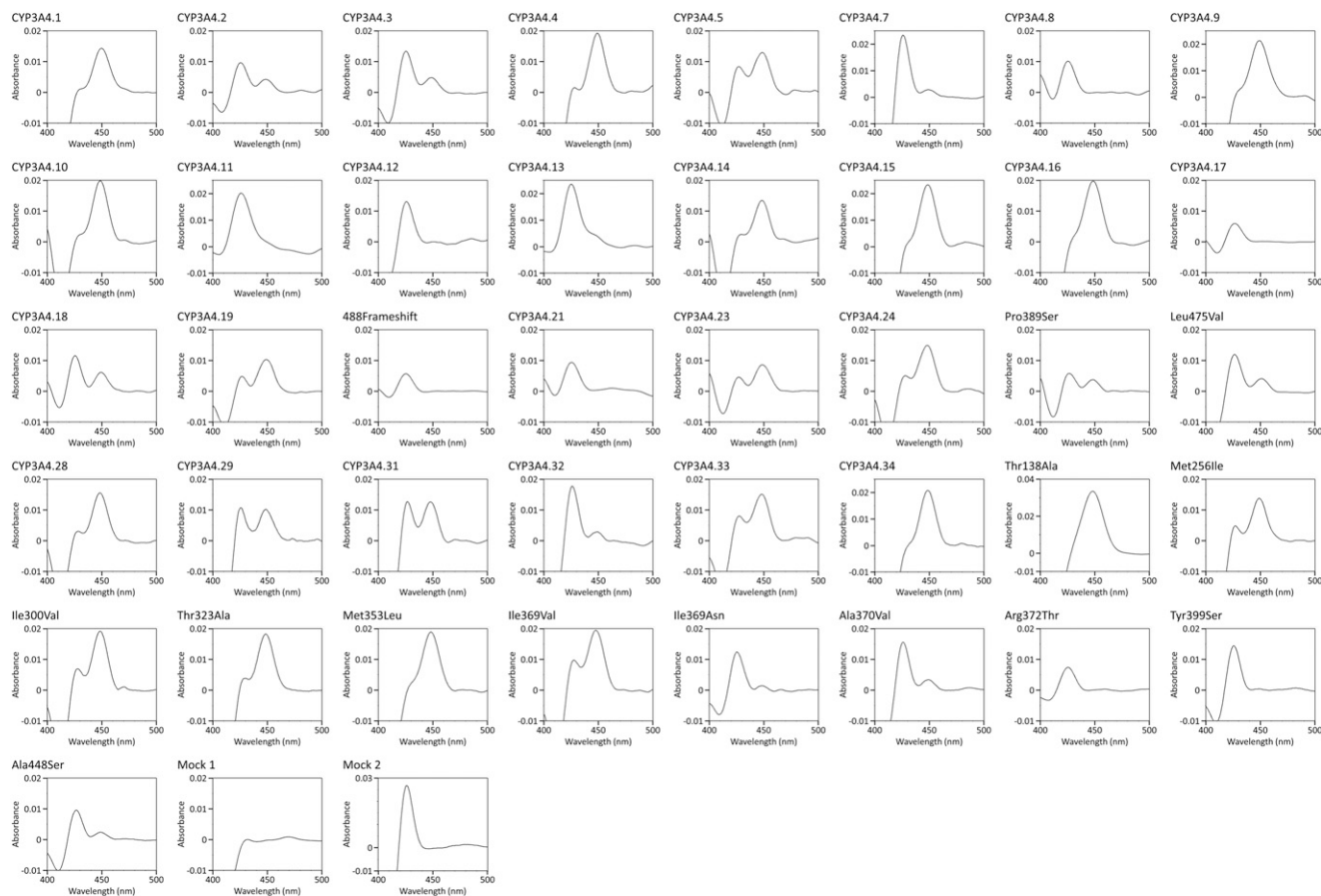


**Fig. 1.** Representative CO-difference spectra of CYP3A4 variant proteins expressed in 293FT cells. All assays and measurements were performed in triplicate using a single microsomal preparation. Mock 1 indicates transfection with 10  $\mu\text{g}$  mock plasmids. Mock 2 indicates transfection with 9.6  $\mu\text{g}$  mock plasmids, 0.2  $\mu\text{g}$  CPR plasmids, and 0.2  $\mu\text{g}$  cytochrome  $b_5$  plasmids.

c.1342C>T variant, were identified among 4773 Japanese individuals with low allele frequencies (0.01%–0.05%).

CYP3A4 protein levels normalized by total protein concentrations were assessed by Western blotting with a polyclonal CYP3A4 antibody that recognized all CYP3A4 variants (Supplemental Figs. 2, A and B). The protein levels of CYP3A4.1 and the CYP3A4 variants did not differ significantly (Supplemental Fig. 2C). Moreover, the aspect ratio of CPR activity and cytochrome  $b_5$  content did not significantly vary among the analyzed CYP3A4 variants (Supplemental Fig. 3). Thus, we used single microsomes expressed per CYP3A4 variant for functional characterization.

In our study, CYP3A4 exhibited high activity with no significant solvent effects. The holoprotein content of CYP3A4 variants expressed in 293FT cells was assessed by CO-difference spectroscopy (Fig. 1). The reduced CO-difference spectra of microsomal fractions of CYP3A4.1 and 31 CYP3A4 variants (CYP3A4.2–.5, .7, .9, .10, .14–.16, .18, .19, .23, .24, Pro389Ser, Leu475Val, .28, .29, .31–.34, Thr138Ala, Met256Ile, Ile300Val, Thr323Ala, Met353Leu, Ile369Val, Ile369Asn, Ala370Val, and Ala448Ser) were determined by measuring the increase in maximum absorption at 450 nm after CO treatment. The remaining nine variants (CYP3A4.8, .11–.13, .17, 488Frameshift, .21, Arg372Thr, and Tyr399Ser) had no detectable holoprotein content based on the lack of a significant increase in their maximum absorption at 450 nm.

We selected midazolam and testosterone as substrates because midazolam 1'-hydroxylation and testosterone 6 $\beta$ -hydroxylation have long been recognized as CYP3A member-mediated reactions. First, we confirmed that the formation of 1'-hydroxymidazolam or 6 $\beta$ -hydroxytestosterone

was linear for up to 10 minutes of incubation by using 50  $\mu\text{g}$  microsomal proteins and 15  $\mu\text{M}$  midazolam or 500  $\mu\text{M}$  testosterone, respectively. Both metabolites were linear in the presence of 0–50  $\mu\text{g}$  microsomal proteins during 10 minutes of incubation. The kinetic parameters were calculated by Michaelis-Menten curves of midazolam 1'-hydroxylation and testosterone 6 $\beta$ -hydroxylation for wild-type CYP3A4 and CYP3A4 variants (Fig. 2; Table 2). However, because of the insufficient metabolite production, we could not determine the kinetic parameters of midazolam 1'-hydroxylation for 11 variants (CYP3A4.8, .11–.13, .17, 488Frameshift, .21, Ile369Asn, Ala370Val, Arg372Thr, and Tyr399Ser). We found that 15 variants had significantly lower catalytic efficiency values ( $P < 0.05$ ) than CYP3A4.1, whereas there were no significant differences in  $K_m$  and  $k_{cat}$  values among these CYP3A4 variants. Conversely, the  $K_m$  values of testosterone 6 $\beta$ -hydroxylation were significantly higher for CYP3A4.7, .16, .33, and Thr138Ala than for CYP3A4.1 ( $P < 0.05$ ). Moreover, the  $k_{cat}$  and catalytic efficiency values were significantly lower for CYP3A4.12 and Leu475Val than for CYP3A4.1 ( $P < 0.05$ ). Insufficient metabolite production prevented us from determining the kinetic values for nine variants (CYP3A4.8, .11, .13, .17, 488Frameshift, .21, Ile369Asn, Ala370Val, and Arg372Thr). Lastly, we calculated the correlation between the midazolam 1'-hydroxylation and the testosterone 6 $\beta$ -hydroxylation catalytic efficiency values. As shown in Fig. 3, there was a significant correlation between these values among the different variants ( $R^2 = 0.724$ ,  $P < 0.001$ ).

We used 3D structural modeling to assess the molecular properties of CYP3A4 variants and their interactions with midazolam. As shown in Fig. 4, A and B, the residue substitution in CYP3A4.8 and CYP3A4.12

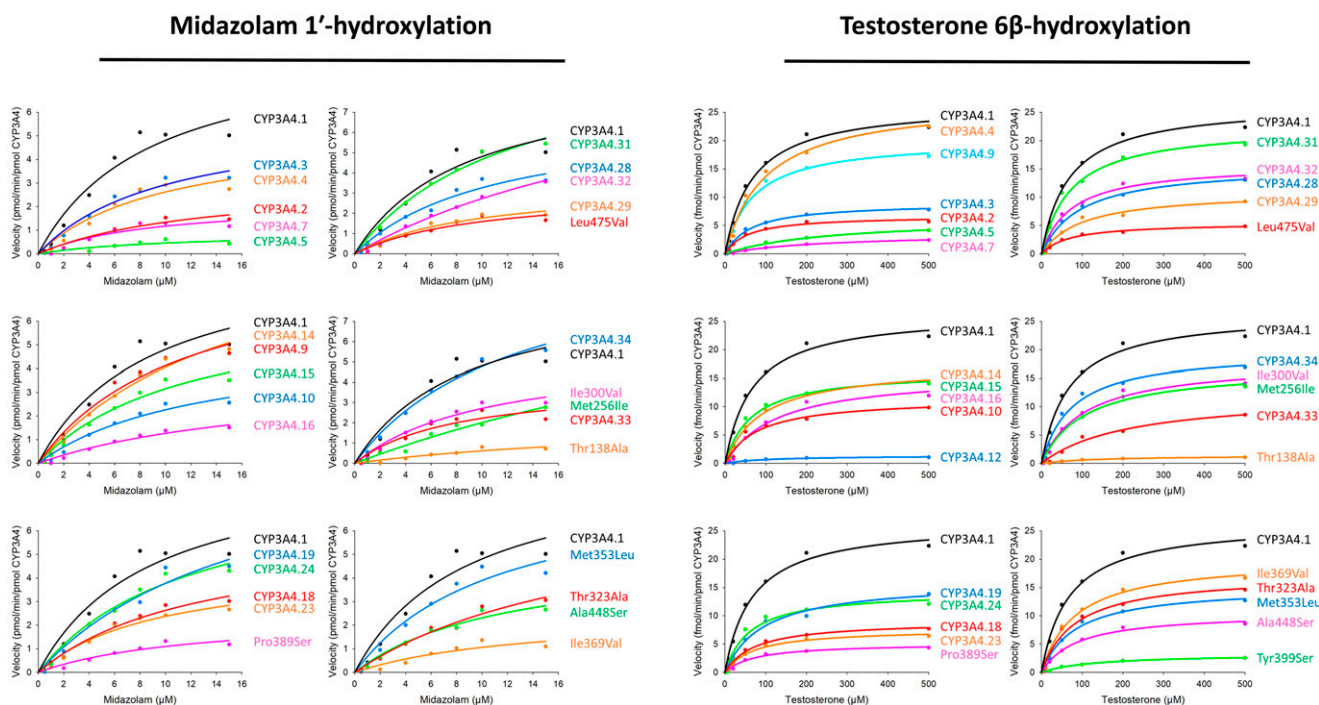


**Fig. 2.** Michaelis-Menten curves for CYP3A4 variants. Determined kinetic parameters ( $K_m$ ,  $k_{cat}$ , and catalytic efficiency) of midazolam 1'-hydroxylation and testosterone 6 $\beta$ -hydroxylation. All assays and measurements were performed in triplicate using a single microsomal preparation.

abolished the interaction with heme. The midazolam docking analysis indicated that the Thr138Ala substitution variant caused a hydrophobic interaction between Arg130 and Ser134 via the adjacently formed hydrophobic interaction between Ala138 and Ser134 (Fig. 4C). In CYP3A4.17, the substitution Ser189 located at the F-G loop lacked a hydrophobic interaction with Leu249 (Fig. 4D). CYP3A4.21 harbored its substitution in the I-helix, which formed a hydrophobic interaction between Cys319 and Val489 (Fig. 4E). Additionally, the substitution Ala448Ser abolished numerous hydrophobic interactions with heme (Fig. 4F). The substitution Tyr399Ser caused the formation of a hydrogen bond with Met371 (Fig. 4G). We further analyzed Ile369 and Val370, as shown in Fig. 4, H–M. The Ile369Val substitution had an additional hydrophobic interaction with midazolam and heme, affecting the distance between heme and the active site (Fig. 4H). Furthermore, differences in the midazolam and heme interactions due to the amino acid substitutions (Fig. 4, I, K, and L), as well as substrate-specific differences in the heme-surrounding interactions (Fig. 4, H, J, K, and M), were observed.

## Discussion

Several CYP3A4 genetic variations may contribute to interindividual differences in drug efficacy and adverse-effect rates (Lamba et al., 2002a). Several studies have identified CYP3A4 variants and characterized the associated in vitro enzyme kinetics, including previous studies of CYP3A4 variants among the Han Chinese population using numerous substrates (Supplemental Table 3) (Fang et al., 2017; Xu et al., 2018; Li et al., 2019a,b; Lin et al., 2019a,b; Yang et al., 2019; Zhou et al., 2019a; Chen et al., 2020). However, the underlying causes for functional differences produced by the amino acid alterations are not fully understood and require further research. This study characterized 40 CYP3A4 variants, including 11 novel variants identified among 4773 Japanese individuals, by assessing CO-difference spectra, enzymatic activities, and 3D structural modeling analysis.

A single individual had two allelic variants (CYP3A4.8 and Thr138Ala, Supplemental Fig. 1), each displaying significantly decreased CYP3A4

activity for midazolam and testosterone. These substitutions were located near the vital CPR-cytochrome P450 electron transfer site, where they could affect the enzymatic activities (Hasemann et al., 1995; Bridges et al., 1998). Accordingly, an increase in the maximum absorption at 450 nm after CO treatment was observed for the Thr138Ala variant (Fig. 1) as a result of interactions involving Ala138 that caused hydrogen bonds between Arg130 and Ser134, which could affect electron transfer because Arg130 located in the C-D loop plays an essential role in electrostatic interactions (Fig. 4C). Interestingly, CYP3A4.8 did not have an absorption peak at 450 nm after CO treatment (Fig. 1), reflecting a failed heme incorporation and resulting in zero CYP3A4.8 holoprotein content that could be based on disrupted interactions with heme (Fig. 4A). Although it may be an infrequent case, carriers of two allelic variants that are predicted to be poor metabolizers may be at an increased risk of adverse drug reactions when treated with drugs metabolized by CYP3A4.

The midazolam and testosterone hydroxylation activities were slightly decreased or absent in 11 variants (CYP3A4.8, .11–.13, .17, 488Frameshift, .21, Ile369Asn, Ala370Val, Arg372Thr, and Tyr399Ser). Excluding Ile369Asn and Ala370Val, the nine remaining variants did not exhibit absorption peaks at 450 nm after CO treatment (Fig. 1), indicating failed heme incorporation. These findings suggest that the remaining nine CYP3A4 variants lacked quantifiable enzymatic activity. Similarly, the zero holoprotein content for variants CYP3A4.8 and CYP3A4.12 may be explained by disrupted interactions with heme (Fig. 4, A and B). The lack of activity exhibited by 488Frameshift was due to extensive changes in its molecular conformation caused by the frameshift mutation. The substitutions in CYP3A4.11 and .13, which were located in the conserved glutamine-arginine-arginine motif and K region critical for maintaining the structure among cytochrome P450 isoforms, could affect holoprotein stability, as previously reported (Eiselt et al., 2001). The substitution in CYP3A4.17 located in the E-helix was associated with slightly decreased enzymatic activity. Ser189 lacked a hydrophobic interaction with Leu249 (Fig. 4D), resulting in conformational changes in the active site cavity around

TABLE 2

Kinetic parameters of midazolam 1'-hydroxylation and testosterone 6β-hydroxylation by microsomes from 293FT cells expressing wild-type CYP3A4 and variant CYP3A4 proteins

The data represent the means ± S.D. of the three independently performed catalytic assays. All assays and measurements were performed in triplicate using a single microsomal preparation. Mock 1 indicates transfection with 10 μg mock plasmids, Mock 2 indicates transfection with 9.6 μg mock plasmids, 0.2 μg CPR plasmids, and 0.2 μg cytochrome b<sub>5</sub> plasmids.

Variants	Midazolam 1'-Hydroxylation			Testosterone 6β-Hydroxylation		
	$K_m$ μM	$k_{cat}$ pmol/min per picomoles CYP3A4	Catalytic Efficiency ( $k_{cat}/K_m$ )	$K_m$ μM	$k_{cat}$ fmol/min per picomoles CYP3A4	Catalytic Efficiency ( $k_{cat}/K_m$ )
CYP3A4.1	2.96 ± 0.19	4.79 ± 0.13	1.63 ± 0.11	67.5 ± 7.15	26.6 ± 1.77	0.40 ± 0.02
CYP3A4.2	3.49 ± 1.12	1.43 ± 0.14	0.45 ± 0.13* (27.4)	55.7 ± 6.88	6.75 ± 0.37*	0.12 ± 0.01*** (30.9)
CYP3A4.3	3.15 ± 0.15	3.00 ± 0.21	0.95 ± 0.04 (58.4)	63.8 ± 6.23	8.41 ± 1.12*	0.13 ± 0.01*** (33.2)
CYP3A4.4	3.56 ± 0.14	2.78 ± 0.09	0.78 ± 0.03 (47.9)	98.9 ± 7.36	27.3 ± 1.49	0.28 ± 0.01* (69.7)
CYP3A4.5	7.64 ± 2.99	0.75 ± 0.09	0.11 ± 0.03* (6.7)	256 ± 23.3	6.37 ± 0.55*	0.02 ± 0.00** (6.3)
CYP3A4.7	4.20 ± 0.36	1.37 ± 0.09	0.33 ± 0.04* (20.2)	240 ± 11.1***	3.63 ± 0.03*	0.02 ± 0.00** (3.8)
CYP3A4.8	N.D.	N.D.	N.D.	N.D.	N.D.	N.D.
CYP3A4.9	3.36 ± 0.11	4.23 ± 0.08	1.26 ± 0.05 (77.5)	68.2 ± 1.43	20.2 ± 0.34	0.30 ± 0.01 (74.8)
CYP3A4.10	4.11 ± 0.34	2.50 ± 0.01	0.61 ± 0.05* (37.6)	103 ± 8.67	12.1 ± 0.22	0.12 ± 0.01*** (29.9)
CYP3A4.11	N.D.	N.D.	N.D.	N.D.	N.D.	N.D.
CYP3A4.12	N.D.	N.D.	N.D.	152 ± 13.4	1.69 ± 0.10*	0.01 ± 0.00** (2.8)
CYP3A4.13	N.D.	N.D.	N.D.	N.D.	N.D.	N.D.
CYP3A4.14	3.97 ± 0.43	4.31 ± 0.28	1.10 ± 0.11 (67.2)	92.2 ± 17.3	17.4 ± 0.98	0.19 ± 0.03* (48.9)
CYP3A4.15	3.46 ± 0.21	3.29 ± 0.15	0.95 ± 0.02 (58.4)	65.5 ± 2.48	15.9 ± 0.09	0.25 ± 0.01* (63.3)
CYP3A4.16	5.51 ± 0.37	1.60 ± 0.07	0.29 ± 0.01* (17.8)	128 ± 4.74*	15.9 ± 0.31	0.12 ± 0.01** (31.5)
CYP3A4.17	N.D.	N.D.	N.D.	N.D.	N.D.	N.D.
CYP3A4.18	3.69 ± 0.27	2.80 ± 0.03	0.76 ± 0.07* (46.9)	73.8 ± 3.85	9.07 ± 0.40*	0.12 ± 0.00* (31.1)
CYP3A4.19	3.97 ± 0.06	4.05 ± 0.14	1.02 ± 0.02 (62.6)	99.5 ± 20.4	16.3 ± 0.48	0.17 ± 0.03 (43.1)
488Frameshift	N.D.	N.D.	N.D.	N.D.	N.D.	N.D.
CYP3A4.21	N.D.	N.D.	N.D.	N.D.	N.D.	N.D.
CYP3A4.22	3.28 ± 0.37	2.48 ± 0.11	0.76 ± 0.05 (46.7)	69.8 ± 1.81	7.66 ± 0.22*	0.11 ± 0.00* (27.7)
CYP3A4.23	3.27 ± 0.38	3.84 ± 0.08	1.19 ± 0.12 (73.0)	63.1 ± 10.7	14.5 ± 0.52	0.23 ± 0.03** (59.2)
CYP3A4.24	4.44 ± 0.37	1.31 ± 0.02	0.30 ± 0.03* (18.2)	73.5 ± 4.84	5.16 ± 0.08*	0.07 ± 0.00** (17.8)
Pro389Ser	3.83 ± 0.17	1.77 ± 0.04	0.46 ± 0.01* (28.4)	68.8 ± 3.80	5.47 ± 0.01*	0.08 ± 0.00** (20.1)
Leu475Val	3.15 ± 0.25	3.32 ± 0.19	1.06 ± 0.09 (65.0)	96.1 ± 8.18	15.7 ± 0.58	0.16 ± 0.01*** (41.5)
CYP3A4.28	3.56 ± 0.33	1.91 ± 0.04	0.54 ± 0.06* (33.2)	98.3 ± 8.96	11.0 ± 0.36	0.11 ± 0.01** (28.4)
CYP3A4.29	3.25 ± 0.42	4.72 ± 0.19	1.47 ± 0.18 (90.4)	72.6 ± 8.08	22.7 ± 1.27	0.31 ± 0.02 (79.4)
CYP3A4.31	5.33 ± 0.47	3.23 ± 0.13	0.61 ± 0.06* (37.5)	73.7 ± 3.36	15.9 ± 0.40	0.22 ± 0.01* (54.6)
CYP3A4.32	3.02 ± 0.16	2.30 ± 0.12	0.76 ± 0.08* (46.9)	214 ± 3.35***	12.3 ± 0.33	0.06 ± 0.00* (14.5)
CYP3A4.33	3.35 ± 0.50	4.86 ± 0.12	1.48 ± 0.21 (91.0)	75.3 ± 3.87	19.9 ± 0.13	0.26 ± 0.01* (66.8)
CYP3A4.34	10.2 ± 0.97	1.10 ± 0.06	0.11 ± 0.01* (6.7)	134 ± 6.81*	1.39 ± 0.00*	0.01 ± 0.00** (2.6)
Thr138Ala	6.87 ± 0.87	2.66 ± 0.13	0.39 ± 0.06* (24.2)	105 ± 4.88	17.0 ± 0.91	0.16 ± 0.00* (40.7)
Met256Ile	3.33 ± 0.49	2.82 ± 0.15	0.86 ± 0.08 (52.8)	105 ± 5.62	18.0 ± 0.48	0.17 ± 0.00* (43.4)
Ile300Val	4.45 ± 0.44	2.79 ± 0.21	0.63 ± 0.02 (38.6)	83.8 ± 7.36	17.3 ± 0.79	0.21 ± 0.01** (52.5)
Thr323Ala	3.33 ± 0.13	4.00 ± 0.10	1.20 ± 0.03 (73.7)	83.9 ± 5.34	15.2 ± 0.44	0.18 ± 0.01** (45.9)
Met353Leu	5.26 ± 0.34	1.34 ± 0.05	0.26 ± 0.01* (15.7)	83.7 ± 5.78	20.1 ± 0.79	0.24 ± 0.01* (60.7)
Ile369Val	N.D.	N.D.	N.D.	N.D.	N.D.	N.D.
Ile369Asn	N.D.	N.D.	N.D.	N.D.	N.D.	N.D.
Ala370Val	N.D.	N.D.	N.D.	N.D.	N.D.	N.D.
Arg372Thr	N.D.	N.D.	N.D.	N.D.	N.D.	N.D.
Tyr399Ser	N.D.	N.D.	N.D.	131 ± 15.7	3.29 ± 0.28*	0.03 ± 0.00** (6.4)
Ala448Ser	3.58 ± 0.35	2.45 ± 0.10	0.69 ± 0.05* (42.4)	85.6 ± 10.9	10.6 ± 1.32*	0.12 ± 0.00* (31.2)
Mock 1	N.D.	N.D.	N.D.	N.D.	N.D.	N.D.
Mock 2	N.D.	N.D.	N.D.	N.D.	N.D.	N.D.

N.D., not determined.

\* $P < 0.05$ ; \*\* $P < 0.01$ ; \*\*\* $P < 0.005$  compared with CYP3A4.1 by Dunnett's T3 test. Catalytic efficiency percentages versus wild-type are indicated in parentheses.



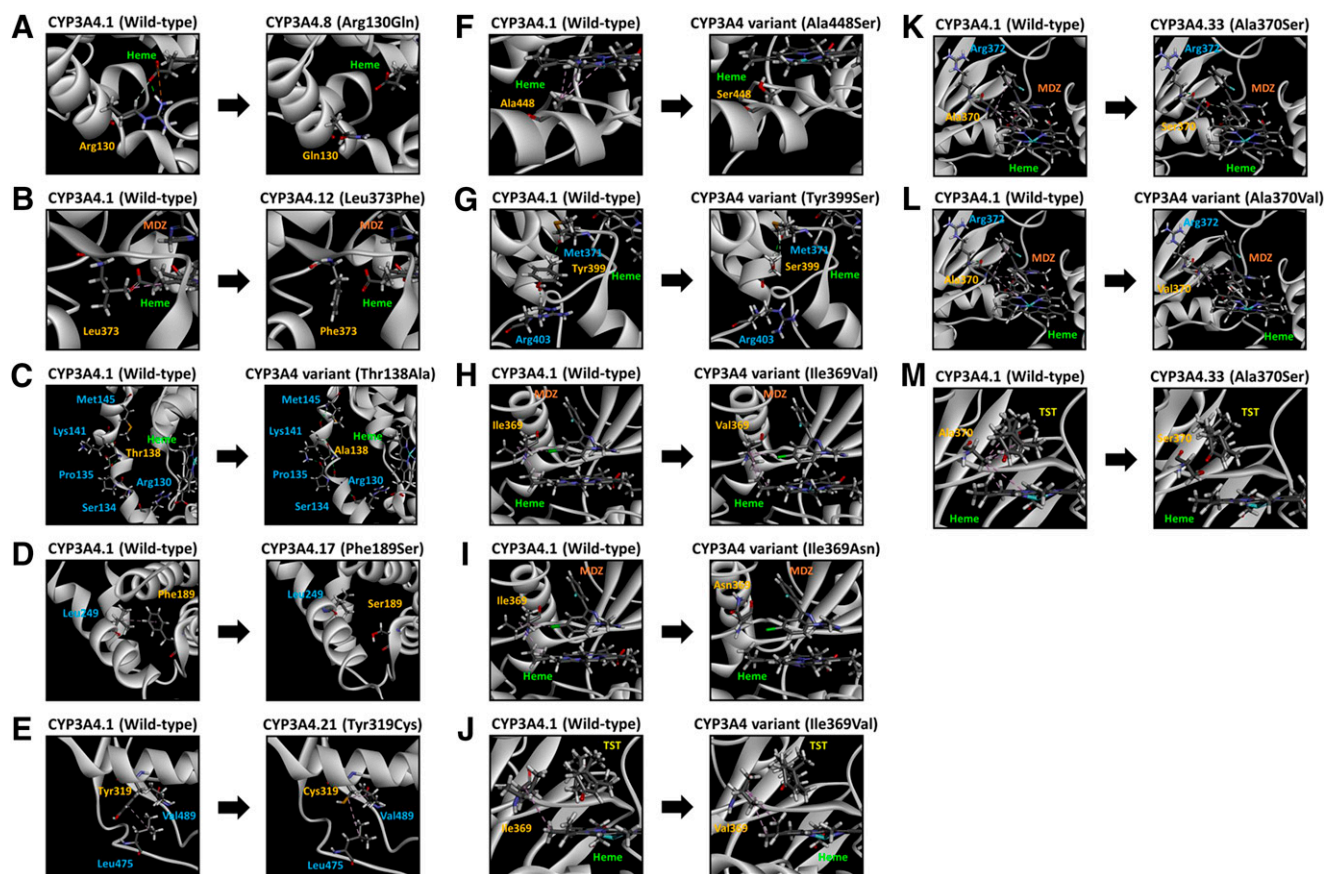


**Fig. 4.** Diagram pairs showing the partial crystal structure of CYP3A4.1 (left image) and CYP3A4 variants (right image) for CYP3A4.8 (A), CYP3A4.12 (B), Thr138Ala (C), CYP3A4.17 (D), CYP3A4.21 (E), Ala448Ser (F), Tyr399Ser (G), Ile369Val coordinated with midazolam (H), Ile369Asn (I), Ile369Val coordinated with testosterone (J), CYP3A4.33 coordinated with midazolam (K), Ala370Val (L), and CYP3A4.33 coordinated with testosterone (M). Pink line, hydrophobic interactions. Green line, conventional hydrogen bonds. Gray line, carbon-hydrogen bonds. MDZ, midazolam; TST, testosterone.

Cytochrome P450 variant characterization by assessing the enzymatic activities for all metabolites and using all possible substrates may prove essential to evaluate the impact caused by amino acid substitutions and to improve treatment outcomes. However, previously developed computational calculations have been successful in predicting the activities of over 90% of representative cytochrome P450 variants (Zhou et al., 2019b). Hence, using computational prediction to assess the effect of amino acid substitutions on enzymatic cytochrome P450 activities may be an acceptable surrogate approach, considering the challenging nature of *in vitro* and *in vivo* analyses.

In summary, we determined the *in vitro* metabolic activities of wild-type CYP3A4 and 40 CYP3A4 variant proteins using our recently established heterologous expression system. These data reveal the functional effects caused by CYP3A4 genetic polymorphisms, including 11 novel variants identified among 4773 Japanese individuals, and have been generated using a single microsomal protein preparation per CYP3A4 variant to reveal their qualitative features. We recognize the limitations associated with a single biologic replicate, and additional biologic replicates would provide greater confidence in estimates of intrinsic clearance for use in future applications. Reduced activity or inactive variants caused by CYP3A4 allelic variations located in the coding region may be the underlying cause of an altered therapeutic response leading to poor treatment outcomes. However, our assay that uses a cDNA-based expression system cannot evaluate the influence of splicing variants. Therefore, further studies including additional biologic replicates as well as the use of minigenes to assess the potential functional consequences of variants affecting splice sites on catalytic

activity are required prior to further downstream applications such as *in vitro-in vivo* extrapolation. In the future, CYP3A4 genetic polymorphisms should be used in combination with other factors affecting the *in vivo* activity of CYP3A4, such as CYP3A4 inducers and inhibitors and CYP3A5 activity, to aid the implementation of personalized medicine, individualized dosing regimens, and predictive risk panels. Our current findings should provide guidance in advancing these efforts.

#### Acknowledgments

We thank the Biomedical Research Core at the Tohoku University Graduate School of Medicine for their technical support. We would like to thank Mizuguchi (Graduate School of Pharmaceutical Sciences, Osaka University) for gifting the plasmid vector. We would like to thank Editage ([www.editage.com](http://www.editage.com)) for English language editing.

#### Authorship Contributions

*Participated in research design:* Kumondai, Hiratsuka.  
*Conducted experiments:* Kumondai, Gutiérrez Rico, Hishinuma, Ueda, Saito, Abe, Maekawa.  
*Contributed new reagents or analytic tools:* Saigusa, Kinoshita, Maekawa, Mano, Hirasawa, Hiratsuka.  
*Performed data analysis:* Kumondai, Saito, Tadaka, Nakayoshi, Oda, Hiratsuka.  
*Wrote or contributed to the writing of the manuscript:* Kumondai, Gutiérrez Rico, Hiratsuka.

#### References

Apellániz-Ruiz M, Lee MY, Sánchez-Barroso L, Gutiérrez-Gutiérrez G, Calvo I, García-Estévez L, Sereno M, García-Donás J, Castelo B, Guerra E, et al. (2015) Whole-exome sequencing reveals



- defective CYP3A4 variants predictive of paclitaxel dose-limiting neuropathy. *Clin Cancer Res* 21:322–328.
- Benkaidali L, André F, Moroy G, Tangour B, Maurel F, and Petitjean M (2019) Four major channels detected in the cytochrome P450 3A4: A Step toward understanding its multispecificity. *Int J Mol Sci* 20:987.
- Bridges A, Gruenke L, Chang YT, Vakser IA, Loew G, and Waskell L (1998) Identification of the binding site on cytochrome P450 2B4 for cytochrome b5 and cytochrome P450 reductase. *J Biol Chem* 273:17036–17049.
- Chen B, Zhang XD, Wen J, Zhang B, Chen D, Wang S, Cai JP, and Hu GX (2020) Effects of 26 recombinant CYP3A4 variants on brexpiprazole metabolism. *Chem Res Toxicol* 33:172–180.
- Christensen H, Mathiesen L, Postvoll LW, Winther B, and Molden E (2009) Different enzyme kinetics of midazolam in recombinant CYP3A4 microsomes from human and insect sources. *Drug Metab Pharmacokin* 24:261–268.
- Clark DP and Pazdernik NJ (2016) *Biotechnology*, Elsevier/AP Cell, Amsterdam.
- Eisele R, Domanski TL, Zibat A, Mueller R, Presecan-Siedel E, Hustert E, Zanger UM, Brockmoller J, Klenk HP, Meyer UA, et al. (2001) Identification and functional characterization of eight CYP3A4 protein variants. *Pharmacogenetics* 11:447–458.
- Ekström L, Skilving I, Ovesjö ML, Aklilu E, Nylén H, Rane A, Diczfalusi U, and Björkhem-Bergman L (2015) miRNA-27b levels are associated with CYP3A activity in vitro and in vivo. *Pharmacol Res Perspect* 3:e00192.
- Elsens L, van Gelder T, Hesselink DA, Hauffroid V, and van Schaik RH (2013) CYP3A4\*22: promising newly identified CYP3A4 variant allele for personalizing pharmacotherapy. *Pharmacogenomics* 14:47–62.
- El Mahjoub A and Staub C (2000) High-performance liquid chromatographic method for the determination of benzodiazepines in plasma or serum using the column-switching technique. *J Chromatogr B Biomed Sci Appl* 742:381–390.
- Fang P, Tang PF, Xu RA, Zheng X, Wen J, Bao SS, Cai JP, and Hu GX (2017) Functional assessment of CYP3A4 allelic variants on lidocaine metabolism in vitro. *Drug Des Devel Ther* 11:3503–3510.
- Foti RS, Rock DA, Wienkers LC, and Wahlstrom JL (2010) Selection of alternative CYP3A4 probe substrates for clinical drug interaction studies using in vitro data and in vivo simulation. *Drug Metab Dispos* 38:981–987.
- Fujikura K, Ingelman-Sundberg M, and Lauschke VM (2015) Genetic variation in the human cytochrome P450 supergene family. *Pharmacogenet Genomics* 25:584–594.
- Fukushima-Uesaka H, Saito Y, Watanabe H, Shiseki K, Saeki M, Nakamura T, Kurose K, Sai K, Komamura K, Ueno K, et al. (2004) Haplotypes of CYP3A4 and their close linkage with CYP3A5 haplotypes in a Japanese population. *Hum Mutat* 23:100.
- Gómez-Bravo MA, Apellaniz-Ruiz M, Salcedo M, Fondevila C, Suarez F, Castellote J, Rufian S, Pons JA, Bilbao I, Alamo JM, et al. (2018) Influence of donor liver CYP3A4\*20 loss-of-function genotype on tacrolimus pharmacokinetics in transplanted patients. *Pharmacogenet Genomics* 28:41–48.
- Gutiérrez Rico EM, Kikuchi A, Saito T, Kumondai M, Hishinuma E, Kaneko A, Chan CW, Gitaka J, Nakayoshi T, Oda A, et al. (2020) CYP2D6 genotyping analysis and functional characterization of novel allelic variants in a Ni-Vanuatu and Kenyan population by assessing dextromethorphan O-demethylation activity. *Drug Metab Pharmacokin* 35:89–101.
- Hasemann CA, Kurumbail RG, Boddupalli SS, Peterson JA, and Deisenhofer J (1995) Structure and function of cytochromes P450: a comparative analysis of three crystal structures. *Structure* 3: 41–62.
- Hendriks DFG, Vorrink SU, Smutny T, Sim SC, Nordling Å, Ullah S, Kumondai M, Jones BC, Johansson I, Andersson TB, et al. (2020) Clinically relevant cytochrome P450 3A4 induction mechanisms and drug screening in three-dimensional spheroid cultures of primary human hepatocytes. *Clin Pharmacol Ther* 108:844–855.
- Hiratsuka M (2012) In vitro assessment of the allelic variants of cytochrome P450. *Drug Metab Pharmacokin* 27:68–84.
- Hiratsuka M (2016) Genetic polymorphisms and in vitro functional characterization of CYP2C8, CYP2C9, and CYP2C19 allelic variants. *Biol Pharm Bull* 39:1748–1759.
- Hornstein BD, Roman D, Arévalo-Soliz LM, Engewig MA, and Zechiedrich L (2016) Effects of circular DNA length on transfection efficiency by electroporation into HeLa cells. *PLoS One* 11: e0167537.
- Huang SM, Strong JM, Zhang L, Reynolds KS, Nallani S, Temple R, Abraham S, Habet SA, Baweja RK, Burckart GJ, et al. (2008) New era in drug interaction evaluation: US Food and Drug Administration update on CYP enzymes, transporters, and the guidance process. *J Clin Pharmacol* 48:662–670.
- Ingelman-Sundberg M, Mkrtrchian S, Zhou Y, and Lauschke VM (2018) Integrating rare genetic variants into pharmacogenetic drug response predictions. *Hum Genomics* 12:26.
- Jackson KD, Durandis R, and Vergne MJ (2018) Role of cytochrome P450 enzymes in the metabolic activation of tyrosine kinase inhibitors. *Int J Mol Sci* 19:2367.
- Kumondai M, Hishinuma E, Gutiérrez Rico EM, Ito A, Nakanishi Y, Saigusa D, Hirasawa N, and Hiratsuka M (2020) Heterologous expression of high-activity cytochrome P450 in mammalian cells. *Sci Rep* 10:14193.
- Kumondai M, Hosono H, Maekawa M, Yamaguchi H, Mano N, Oda A, Hirasawa N, and Hiratsuka M (2018) Functional characterization of 9 CYP2A13 allelic variants by assessment of nicotine C-oxidation and coumarin 7-hydroxylation. *Drug Metab Pharmacokin* 33:82–89.
- Lamba JK, Lin YS, Schuetz EG, and Thummel KE (2002a) Genetic contribution to variable human CYP3A-mediated metabolism. *Adv Drug Deliv Rev* 54:1271–1294.
- Lamba JK, Lin YS, Thummel K, Daly A, Watkins PB, Strom S, Zhang J, and Schuetz EG (2002b) Common allelic variants of cytochrome P4503A4 and their prevalence in different populations. *Pharmacogenetics* 12:121–132.
- Lee SJ, Bell DA, Coulter SJ, Ghanayem B, and Goldstein JA (2005) Recombinant CYP3A4\*17 is defective in metabolizing the hypertensive drug nifedipine, and the CYP3A4\*17 allele may occur on the same chromosome as CYP3A5\*3, representing a new putative defective CYP3A haplotype. *J Pharmacol Exp Ther* 313:302–309.
- Li YH, Lin QM, Pang NH, Zhang XD, Huang HL, Cai JP, and Hu GX (2019a) Functional characterization of 27 CYP3A4 protein variants to metabolize regorafenib in vitro. *Basic Clin Pharmacol Toxicol* 125:337–344.
- Li YH, Lu XR, Lin QM, Huang HL, Liang XL, Cai JP, Cui J, and Hu GX (2019b) Functional characterization of 27 CYP3A4 variants on macitentan metabolism in vitro. *J Pharm Pharmacol* 71:1677–1683.
- Lin QM, Li YH, Liu Q, Pang NH, Xu RA, Cai JP, and Hu GX (2019a) Functional characteristics of CYP3A4 allelic variants on the metabolism of loperamide in vitro. *Infect Drug Resist* 12:2809–2817.
- Lin QM, Li YH, Lu XR, Wang R, Pang NH, Xu RA, Cai JP, and Hu GX (2019b) Characterization of genetic variation in CYP3A4 on the metabolism of cabozantinib in vitro. *Chem Res Toxicol* 32:1583–1590.
- Maekawa K, Harakawa N, Yoshimura T, Kim SR, Fujimura Y, Aohara F, Sai K, Katori N, Tohkin M, Naito M, et al. (2010) CYP3A4\*16 and CYP3A4\*18 alleles found in East Asians exhibit differential catalytic activities for seven CYP3A4 substrate drugs. *Drug Metab Dispos* 38:2100–2104.
- Murayama N, Nakamura T, Saeki M, Soyama A, Saito Y, Sai K, Ishida S, Nakajima O, Itoda M, Ohno Y, et al. (2002) CYP3A4 gene polymorphisms influence testosterone 6beta-hydroxylation. *Drug Metab Pharmacokin* 17:150–156.
- Nagasaki M, Yasuda J, Katsuoka F, Nariai N, Kojima K, Kawai Y, Yamaguchi-Kabata Y, Yokozawa J, Danjoh I, Saito S, et al. ToMMo Japanese Reference Panel Project (2015) Rare variant discovery by deep whole-genome sequencing of 1,070 Japanese individuals. *Nat Commun* 6:8018.
- Nguyen V, Espiritu M, and Elbarbry F (2020) Development and validation of a sensitive and specific LC-MS/MS cocktail assay for CYP450 enzymes: application to study the effect of catechin on rat hepatic CYP activity. *Biomed Chromatogr* 34:e4789.
- Niwa T, Okamoto A, Narita K, Toyota M, Kato K, Kobayashi K, and Sasaki S (2020) Comparison of steroid hormone hydroxylation mediated by cytochrome P450 3A subfamilies. *Arch Biochem Biophys* 682:108283.
- Niwa T, Yasumura M, Murayama N, and Yamazaki H (2014) Comparison of catalytic properties of cytochromes P450 3A4 and 3A5 by molecular docking simulation. *Drug Metab Lett* 8:43–50.
- Oda A, Yamaotsu N, and Hirono S (2005) New AMBER force field parameters of heme iron for cytochrome P450s determined by quantum chemical calculations of simplified models. *J Comput Chem* 26:818–826.
- Pan YZ, Gao W, and Yu AM (2009) MicroRNAs regulate CYP3A4 expression via direct and indirect targeting. *Drug Metab Dispos* 37:2112–2117.
- Racha JK, Zhao ZS, Olejnik N, Warner N, Chan R, Moore D, and Satoh H (2003) Substrate dependent inhibition profiles of fourteen drugs on CYP3A4 activity measured by a high throughput LCMS/MS method with four probe drugs, midazolam, testosterone, nifedipine and terfenadine. *Drug Metab Pharmacokin* 18:128–138.
- Saito T, Gutiérrez Rico EM, Kikuchi A, Kaneko A, Kumondai M, Akai F, Saigusa D, Oda A, Hirasawa N, and Hiratsuka M (2018) Functional characterization of 50 CYP2D6 allelic variants by assessing primaquine 5-hydroxylation. *Drug Metab Pharmacokin* 33:250–257.
- Sakurai F, Kawabata K, Yamaguchi T, Hayakawa T, and Mizuguchi H (2005) Optimization of adenovirus serotype 35 vectors for efficient transduction in human hematopoietic progenitors: comparison of promoter activities. *Gene Ther* 12:1424–1433.
- Schärfe CPI, Tremmel R, Schwab M, Kohlbacher O, and Marks DS (2017) Genetic variation in human drug-related genes. *Genome Med* 9:117.
- Sevrioukova IF (2017) High-level production and properties of the cysteine-depleted cytochrome P450 3A4. *Biochemistry* 56:3058–3067.
- Sevrioukova IF and Poulos TL (2017) Structural basis for regioselective midazolam oxidation by human cytochrome P450 3A4. *Proc Natl Acad Sci USA* 114:486–491.
- Watanabe T, Saito T, Rico EMG, Hishinuma E, Kumondai M, Maekawa M, Oda A, Saigusa D, Saito S, Yasuda J, et al. (2018) Functional characterization of 40 CYP2B6 allelic variants by assessing efavirenz 8-hydroxylation. *Biochem Pharmacol* 156:420–430.
- Werk AN, Lefeldt S, Bruckmueller H, Hemmrich-Stanisak G, Franke A, Roos M, Küchle C, Steubl D, Schmaderer C, Bräsen JH, et al. (2014) Identification and characterization of a defective CYP3A4 genotype in a kidney transplant patient with severely diminished tacrolimus clearance. *Clin Pharmacol Ther* 95:416–422.
- Xiao K, Gao J, Weng SJ, Fang Y, Gao N, Wen Q, Jin H, and Qiao HL (2019) CYP3A4/5 activity probed with testosterone and midazolam: correlation between two substrates at the microsomal and enzyme levels. *Mol Pharm* 16:382–392.
- Xu RA, Wen J, Tang P, Wang C, Xie S, Zhang BW, Zhou Q, Cai JP, and Hu GX (2018) Functional characterization of 22 CYP3A4 protein variants to metabolize ibuprofen in vitro. *Basic Clin Pharmacol Toxicol* 122:383–387.
- Yamamoto T, Nagafuchi N, Ozeki T, Kubota T, Ishikawa H, Ogawa S, Yamada Y, Hirai H, and Iga T (2003) CYP3A4\*18: it is not rare allele in Japanese population. *Drug Metab Pharmacokin* 18:267–268.
- Yang CC, Zheng X, Liu TH, Wang CC, Tang PF, Chen Z, Zhang BW, Fang P, Hu GX, and Cai JP (2019) Functional characterization of 21 CYP3A4 variants on amiodarone metabolism in vitro. *Xenobiotica* 49:120–126.
- Zanger UM, Momoi K, Hofmann U, Schwab M, and Klein K (2020) Tri-allelic haplotypes determine and differentiate functionally normal allele CYP2D6\*2 and impaired allele CYP2D6\*41. *Clin Pharmacol Ther* DOI: 10.1002/cpt.2078 [published ahead of print].
- Zanger UM and Schwab M (2013) Cytochrome P450 enzymes in drug metabolism: regulation of gene expression, enzyme activities, and impact of genetic variation. *Pharmacol Ther* 138: 103–141.
- Zawaira A, Ching LY, Coulson L, Blackburn J, and Wei YC (2011) An expanded, unified substrate recognition site map for mammalian cytochrome P450s: analysis of molecular interactions between 15 mammalian CYP450 isoforms and 868 substrates. *Curr Drug Metab* 12:684–700.
- Zhou XY, Hu XX, Wang CC, Lu XR, Chen Z, Liu Q, Hu GX, and Cai JP (2019a) Enzymatic activities of CYP3A4 allelic variants on quinine 3-hydroxylation in vitro. *Front Pharmacol* 10: 591.
- Zhou Y, Ingelman-Sundberg M, and Lauschke VM (2017) Worldwide distribution of cytochrome P450 alleles: a meta-analysis of population-scale sequencing projects. *Clin Pharmacol Ther* 102: 688–700.
- Zhou Y, Mkrtrchian S, Kumondai M, Hiratsuka M, and Lauschke VM (2019b) An optimized prediction framework to assess the functional impact of pharmacogenetic variants. *Pharmacogenomics J* 19:115–126.

**Address correspondence to:** Dr. Masahiro Hiratsuka, Laboratory of Pharmacotherapy of Life-Style Related Diseases, Graduate School of Pharmaceutical Sciences, Tohoku University, 6-3 Aoba, Aramaki, Aoba-ku, Sendai 980-8578, Japan. E-mail: masahiro.hiratsuka.a8@tohoku.ac.jp

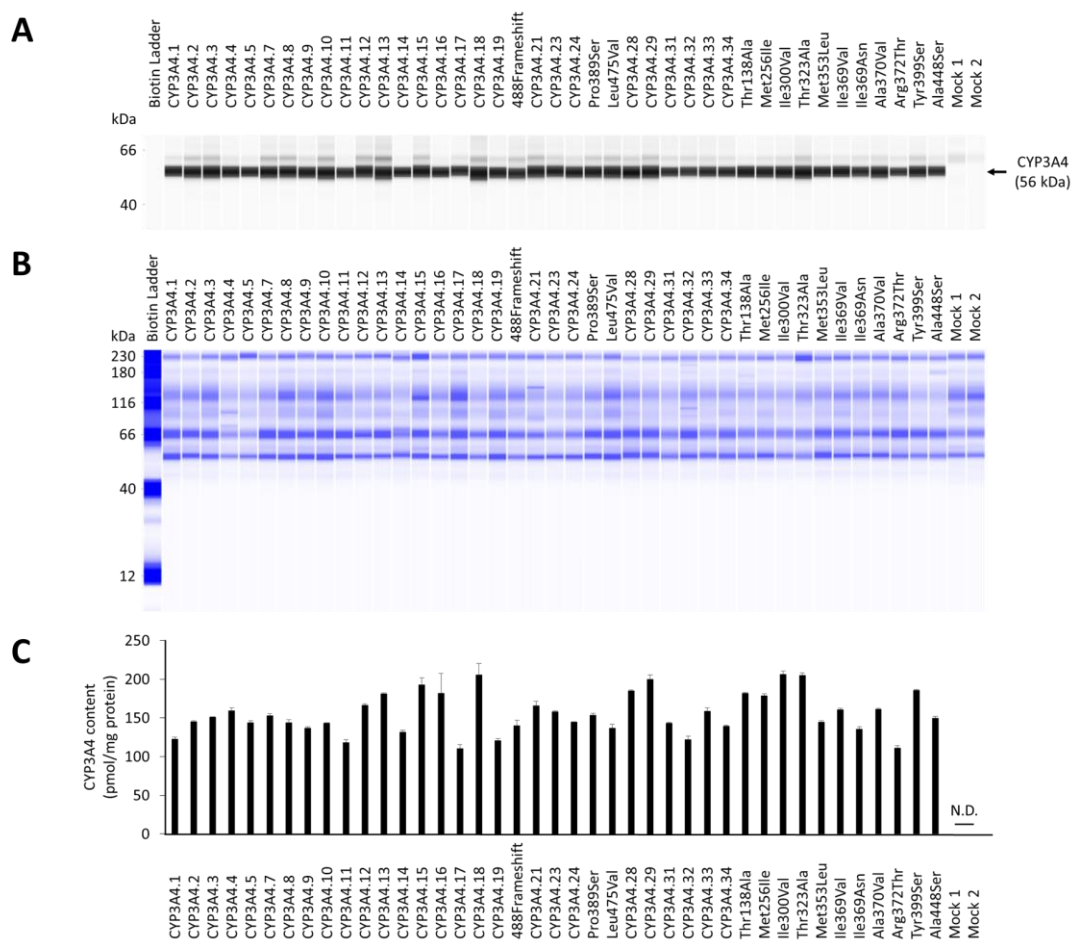
**Supplemental Data**

Functional characterization of 40 CYP3A4 variants by assessing midazolam 1'-hydroxylation and testosterone 6 $\beta$ -hydroxylation

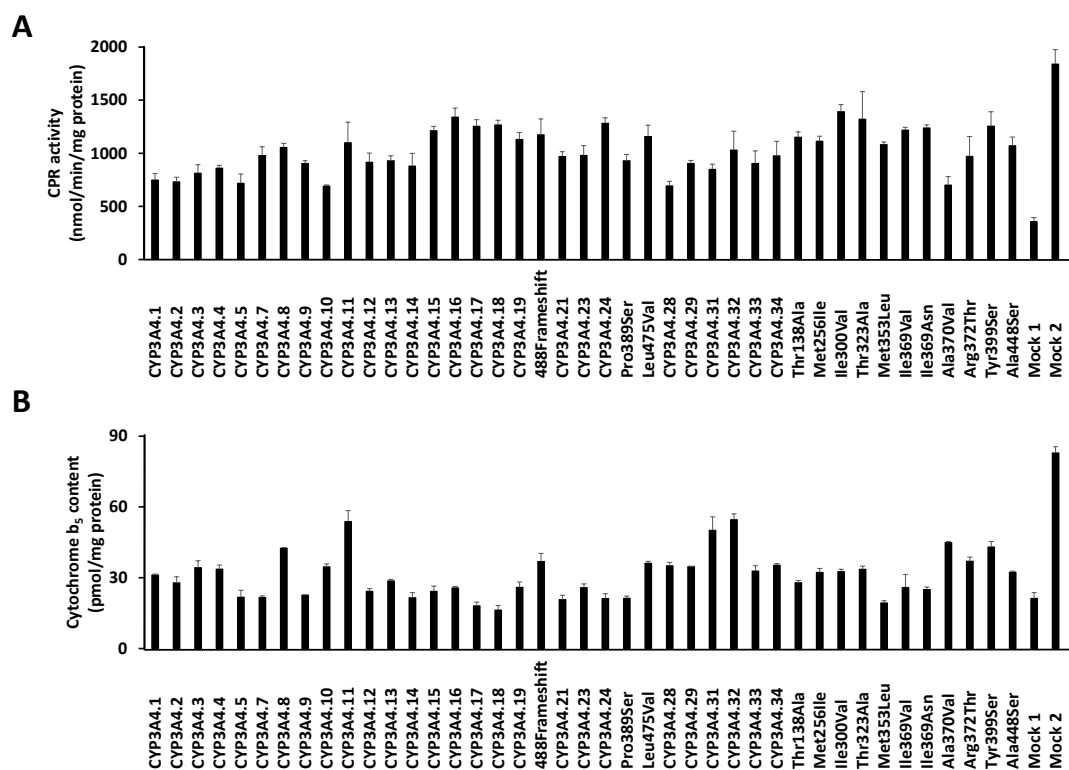
Masaki KUMONDAI, Evelyn Marie GUTIÉRREZ RICO, Eiji HISHINUMA, Akiko UEDA, Sakae SAITO, Daisuke SAIGUSA, Shu TADAKA, Kengo KINOSHITA, Tomoki NAKAYOSHI, Akifumi ODA, Ai ABE, Masamitsu MAEKAWA, Nariyasu MANO, Noriyasu HIRASAWA, Masahiro HIRATSUKA

Drug Metabolism and Disposition





**Supplementary Fig. 2.** Representative western blots showing immunoreactive CYP3A4 proteins (A) and total proteins (B). Average CYP3A4 levels are normalized by total protein content (C). All assays and measurements were performed in triplicates using a single microsomal preparation. Mock 1 indicates transfection with 10  $\mu\text{g}$  mock plasmids. Mock 2 indicates transfection with 9.6  $\mu\text{g}$  mock plasmids, 0.2  $\mu\text{g}$  CPR plasmids, and 0.2  $\mu\text{g}$  cytochrome b<sub>5</sub> plasmids. N.D. represents not determined.



**Supplementary Fig. 3.** Differences of CPR activity (A) and cytochrome b<sub>5</sub> content (B) among microsomal proteins expressed in 293FT cells transfected with plasmids carrying the respective CYP3A4 cDNA. All assays and measurements were performed in triplicates using a single microsomal preparation. Mock 1 indicates transfection with 10  $\mu$ g mock plasmids. Mock 2 indicates transfection with 9.6  $\mu$ g mock plasmids, 0.2  $\mu$ g CPR plasmids, and 0.2  $\mu$ g cytochrome b<sub>5</sub> plasmids.

Supplementary Table 1. PCR primers used to amplify the sequence of the human CYP3A4 gene to confirm the novel allelic variants observed in 4,773 Japanese subjects.

Exon	Size (bp)	Forward Primer (5'-3')	Reverse Primer (5'-3')
1	1285	GATACTATTCCACCAAGCCATCAGC	GAGTTTCACCATGTTAGCCAG
2	444	TCATGGTGGAGGCAGGAAAGG	GAGCCCTTGGGTAAACATTGC
3	517	TCAGTATCCACAACACTTGGAG	GCCTCTTTGTCTTGCTTTACTTCC
4	384	GACTCTTGCTGTGTGTCATACC	GATGAAGTGGACGTGGAACC
5-6	734	CATCACCCAGTAGACAGTCAC	TGGGAGACCCATTGAAGTTG
7	487	GTGGCTGTTTGTCTGTCTTG	GATGACAGGGTTTGTGACAGG
8	462	GCTTCCAGTTGAGAACCTTG	GTGCTGTCTCTGACTCATTCTC
9	457	TCACTGGTGATTCAGGCAAC	AGACCGCAGACTGACTTTCTAG

10	610	GATGGCCCACATTCTCGAAG	AGATGAACCAGAGCCAGCAC
11	937	GAGCACAGCAATGGGCATGAC	TCTCCATCTCTCCCTCTTTCTCC
12	515	CAGGAGAGTAGAAAGGATCTGTAG	CTGAAGCACCCCTTAAAGATCAC
13	963	GGCCTGGCACAGAATAGTAC	CACGCCAACAGTGATTACAATG

---

Supplementary Table 2. Sequences of the primers used for site-directed mutagenesis

	Nucleotide change	Amino acid substitution	Forward Primer (5'-3')	Reverse Primer (5'-3')
<i>CYP3A4*2</i>	664T>C	Ser222Pro	GAGGAATGGAAAGACTGTTA TTGGGAGAAAGAATGGATCC AAAAAAT	ATTTTTTGGATCCATTCTTTCT CCCAATAACAGTCTTTCCATT CCTC
<i>CYP3A4*3</i>	1334T>C	Met445Thr	TCATGAGAGCAAACCTCGTG CCAATGCAGTTTCTG	CAGAAACTGCATTGGCACGA GGTTTGCTCTCATGA
<i>CYP3A4*4</i>	352A>G	Ile118Val	TCATCCTCAGCTATAGAGACG GCACTTTTCATAAATCCC	GGGATTTATGAAAAGTGCCGT CTCTATAGCTGAGGATGA
<i>CYP3A4*5</i>	653C>G	Pro218Arg	GAAAGACTGTTATTGAGAGA	GCTTTTAAGATTTGATTTTTTG



			AAGAATCGATCCAAAAAATC	GATCGATTCTTTCTCTCAATA
			AAATCTTAAAAGC	ACAGTCTTTC
<i>CYP3A4*7</i>	167G>A	Gly56Asp	CATTCCATGTCAAACATACAA	GAAATATTTTGTCTACCATA
			AAGTCCTTATGGTAGGACAA	AGGACTTTTGTATGTTTGACA
			AATATTTC	TGGAATG
<i>CYP3A4*8</i>	389G>A	Arg130Gln	GGTTGGAGACAGCAATGATT	GAAGAATGGAAGAGATTACA
			GTAATCTCTTCCATTCTTC	ATCATTGCTGTCTCCAACC
<i>CYP3A4*9</i>	508G>A	Val170Ile	CTTTCAAGGTGATAGGCTTGC	GGAAGCAGAGACAGGCAAG
			CTGTCTCTGCTTCC	CCTATCACCTTGAAAG
<i>CYP3A4*10</i>	520G>C	Asp174His	CCCAAAGACGTGTTTCAAGG	GGCAAGCCTGTCACCTTGAA
			TGACAGGCTTGCC	ACACGTCTTTGGG

<i>CYP3A4*11</i>	1088C>T	Thr363Met	GGGAATAATCTGAGCATTCA	GTATCTTGACATGGTGGTGAA
			TTCACCACCATGTCAAGATAC	TGAAATGCTCAGATTATTCCC
<i>CYP3A4*12</i>	1117C>T	Leu373Phe	CTTTTTTGCAGACCCTCTCAA	TTATTCCCAATTGCTATGAGAT
			ATCTCATAGCAATTGGGAATA	TTGAGAGGGTCTGCAAAAAA
			A	G
<i>CYP3A4*13</i>	1247C>T	Pro416Leu	GCCTGAGAAGTTCCTCCTTG	TCTTGCTGAATCTTTCAAGGA
			AAAGATTCAGCAAGA	GGAACTTCTCAGGC
<i>CYP3A4*14</i>	44T>C	Leu15Pro	CAGGCTGACAGCCGGGAGAA	ACCTGGCTTCTCCCGGCTGTC
			GCCAGGT	AGCCTG
<i>CYP3A4*15</i>	485G>A	Arg162Gln	GCCTGTCTCTGCTTCCTGCCT	GTGAGAAATCTGAGGCAGGA
			CAGATTTCTCAC	AGCAGAGACAGGC

<i>CYP3A4*16</i>	554C>G	Thr185Ser	CTCCAAATGATGTGCTACTGA TCACATCCATGCTG	CAGCATGGATGTGATCAGTAG CACATCATTGGAG
<i>CYP3A4*17</i>	566T>C	Phe189Ser	GATGTTCACTCCAGATGATGT GCTAGTGATCACATCCAT	ATGGATGTGATCACTAGCACA TCATCTGGAGTGAACATC
<i>CYP3A4*18</i>	878T>C	Leu293Pro	GGCCACGAGCTCCGGATCGG ACAGAGC	GCTCTGTCCGATCCGGAGCTC GTGGCC
<i>CYP3A4*19</i>	1399C>T	Pro467Ser	ATCTGTGTTTCTTTACAAGAT TTGAAGGAGAAGTTCTGAAG GAC	GTCCTTCAGAACTTCTCCTTC AAATCTTGTAAGAAACACA GAT
<i>CYP3A4*20</i>	1461_1462insA	488Frameshift	TTAGAACAACGGGTTTTTTTCT GGTTGAAGAAGTCCTCCT	AGGAGGACTTCTTCAACCAG AAAAAACCCGTTGTTCTAA

<i>CYP3A4*21</i>	956A>G	Tyr319Cys	GTGGCCAGTTCACACATAATG AAGGAGAGAACA CTG	CAGTGTTCTCTCCTTCATTAT GTGTGAACTGGCCAC
<i>CYP3A4*23</i>	484C>T	Arg162Trp	CCTGTCTCTGCTTCCCACCTC AGATTTCTCACC	GGTGAGAAATCTGAGGTGGG AAGCAGAGACAGG
<i>CYP3A4*24</i>	600A>T	Gln200His	GTTTTCCACAAAGGGGTCAT GTGGATTGTTGAGAGAG	CTCTCTCAACAATCCACATGA CCCCTTTGTGGAAAAC
<i>CYP3A4*25</i>	1165C>T	Pro389Ser	CCACCCCTTTGGAAATGAAC ATCCCAT TGATCTCAA	TTGAGATCAATGGGATGTTCA TTTCCAAAGGGGTGG
<i>CYP3A4*27</i>	1423C>G	Leu475Val	CCTCCTAAGCTTAATTTACAG GGGATCTGTGTTTCTTTA	TAAAGAAACACAGATCCCCG TGAAATTAAGCTTAGGAGG
<i>CYP3A4*28</i>	64C>G	Leu22Phe	GGTTCCATATAGATAGACGAG	TGTCAGCCTGGTGCTCGTCTA

			CACCAGGCTGACA	TCTATATGGAACC
<i>CYP3A4*29</i>	337T>A	Phe113Ile	AGATGGCACTTTTCATAATTC	CCTTTTGGTCCAGTGGGAATT
			CCACTGGACCAAAGG	ATGAAAAGTGCCATCT
<i>CYP3A4*31</i>	972C>A	His324Gln	GCTGGACATCAGGTTGAGTG	TGTATGAACTGGCCACTCAAC
			GCCAGTTCATACA	CTGATGTCCAGC
<i>CYP3A4*32</i>	1004T>C	Ile335Thr	CAGAAACTGCAGGAGGAAA	GGGTAAACTGCATCAGTTTC
			CTGATGCAGTTTTACCC	CTCCTGCAGTTTCTG
<i>CYP3A4*33</i>	1108G>T	Ala370Ser	CCCTCTCAAGTCTCATAGAAA	GCTCAGATTATTCCCAATTC
			TTGGAATAATCTGAGC	TATGAGACTTGAGAGGG
<i>CYP3A4*34</i>	1279A>G	Ile427Val	GTGTGTATATGTAAGGATCTA	AGCAAGAAGAACAAGGACA
			CGTTGTCCTTGTTCTTCTTGC	ACGTAGATCCTTACATATACA

		T	CAC
412A>G	Thr138Ala	CTTGAGTTTTTCCACTGGCGA	TGCTGTCTCCAACCTTCGCCA
		AGGTTGGAGACAGCA	GTGGAAACTCAAG
768G>C	Met256Ile	GTATCTTCGAGGCGACTTTCT	TTAAGAAAATCTGTAAAAAG
		TTGATCCTTTTTACAGATTTTC	GATCAAAGAAAGTCGCCTCG
		TTAA	AAGATAC
898A>G	Ile300Val	CCAGCAAAAATAAAGATAAC	GAGCTCGTGGCCCAATCAGT
		TGATTGGGCCACGAGCTC	TATCTTTATTTTGCTGG
967A>G	Thr323Ala	CTGGACATCAGGGTGAGCGG	TTATGTATGAACTGGCCGCTC
		CCAGTTCATACATAA	ACCCTGATGTCCAG
1057A>T	Met353Leu	ACCATGTCAAGATACTCCAAC	CTATGATACTGTGCTACAGTT

		TGTAGCACAGTATCATAG	GGAGTATCTTGACATGGT
1105A>G	Ile369Val	CTCTCAAGTCTCATAGCAACT	AACGCTCAGATTATTCCCAGT
		GGGAATAATCTGAGCGTT	TGCTATGAGACTTGAGAG
1106T>A	Ile369Asn	TCTCAAGTCTCATAGCATTG	GAAACGCTCAGATTATTCCCA
		GGAATAATCTGAGCGTTTC	AATGCTATGAGACTTGAGA
1109C>T	Ala370Val	GACCCTCTCAAGTCTCATAAC	CTCAGATTATTCCCAATTGTT
		AATTGGGAATAATCTGAG	ATGAGACTTGAGAGGGTC
1115G>C	Arg372Thr	GACCCTCTCAAGTGTCATAGC	CTCAGATTATTCCCAATTGCT
		AATTGGGAATAATCTGAG	ATGACACTTGAGAGGGTC
1196A>C	Tyr399Ser	GGTGGTGGTGATGATTCCAA	CGGTGAAGAGCAGAGCTTGG
		GCTCTGCTCTTCACCG	AATCATCACCACCACC

1342G>T

Ala448Ser

CTGCATTGGCATGAGGTTTTC

GTTTCATGTTTCATGAGAGAAA

TCTCATGAACATGAAAC

ACCTCATGCCAATGCAG

---



Supplementary Table 3. Summary of studies on the catalytic efficiency values of CYP3A4 allelic variants identified in the Han Chinese population.

Authors (year)	Fang	Xu	Yang	Li	Li	Lin	Lin	Zhou	Chen	Present study	
	(2017)	(2018)	(2019)	(2019)	(2019)	(2019)	(2019)	(2019)	(2020)		
Substrate	lidocaine	ibrutinib	amiodarone	macitentan	regorafenib	loperamide	cabozantinib	quinine	brepiprazole	midazolam	testosterone
	Catalytic efficiency (% of wild-type)										
	( $\mu\text{L}/\text{min}/\text{pmol}$	( $\text{nL}/\text{min}/\text{pmol}$	( $\mu\text{L}/\text{min}/\text{pmol}$	( $\mu\text{L}/\text{min}/\text{pmol}$	( $\mu\text{L}/\text{min}/\text{pmol}$	( $\mu\text{L}/\text{min}/\text{pmol}$	( $\mu\text{L}/\text{min}/\text{pmol}$	( $\mu\text{L}/\text{min}/\text{pmol}$	( $\text{nL}/\text{min}/\text{pmol}$	( $\mu\text{L}/\text{min}/\text{pmol}$	( $\text{nL}/\text{min}/\text{pmol}$
	CYP3A4)	CYP3A4)	CYP3A4)	CYP3A4)	CYP3A4)	CYP3A4)	CYP3A4)	CYP3A4)	CYP3A4)	CYP3A4)	CYP3A4)
CYP3A4.1	17.0 (100)	47.5 (100)	0.76 (100)	0.06 (100)	1.17 (100)	0.95 (100)	31.2 (100)	217 (100)	44.9 (100)	1.63 (100)	0.40 (100)
CYP3A4.2	4.73 (27.9)	27.3 (57.7)	2.23 (289)	0.08 (131)	0.04 (3.1)	0.07 (7.5)	3.21 (10.3)	32.1 (14.8)	7.4 (16.5)	0.45 (27.4)	0.12 (30.9)
CYP3A4.3	18.0 (107)	69.6 (141)	1.03 (136)	0.13 (209)	0.83 (71.1)	0.32 (33.9)	18.8 (60.2)	49.2 (22.6)	24 (53.5)	0.95 (58.4)	0.13 (33.2)
CYP3A4.4	14.8 (86.0)	56.2 (117)	0.67 (88.9)	0.09 (154.5)	0.66 (57.0)	0.45 (46.9)	26.2 (84.0)	64.8 (29.8)	32.3 (71.9)	0.78 (47.9)	0.28 (69.7)
CYP3A4.5	5.60 (33.0)	38.6 (81.4)	0.77 (102)	0.30 (501)	1.27 (108)	0.45 (47.1)	13.3 (42.6)	22.7 (10.4)	22.5 (50.1)	0.11 (6.7)	0.02 (6.3)

CYP3A4.6						N.D.	N.D.	N.D.			
CYP3A4.7				0.04 (65.2)	0.18 (15.1)	0.37 (38.7)	87.5 (21.4)	26.6 (12.2)	13.2 (29.4)	0.33 (20.2)	0.02 (3.8)
CYP3A4.8				0.06 (102)	0.10 (8.5)	0.68 (71.7)	4.68 (15.0)	5.6 (2.6)	8.2 (18.3)	N.D.	N.D.
CYP3A4.9	11.5 (67.9)	83.4 (171)	1.11 (146)	0.02 (31.8)	0.74 (60.9)	0.13 (13.6)	12.6 (40.2)	40.9 (18.8)	24.4 (54.3)	1.26 (77.5)	0.30 (74.8)
CYP3A4.10	19.1 (110)	46.3 (97.2)	1.59 (210)	0.15 (252)	0.87 (74.2)	0.47 (49.6)	30.1 (96.4)	51.7 (23.8)	34 (75.7)	0.61 (37.6)	0.12 (29.9)
CYP3A4.11	36.4 (214)	40.5 (84.9)	3.34 (436)	0.02 (41.0)	0.14 (11.7)	0.17 (17.5)	15.3 (49.1)	159 (73.5)	16.7 (37.2)	N.D.	N.D.
CYP3A4.12				0.01 (23.1)	0.11 (9.2)	0.24 (25.5)	5.00 (16.0)	5.6 (2.6)	17.2 (38.3)	N.D.	0.01 (2.8)
CYP3A4.13				0.03 (42.1)	0.24 (20.6)	0.11 (11.8)	10.5 (33.7)	12.6 (5.8)	21.1 (47.0)	N.D.	N.D.
CYP3A4.14	25.7 (152)	27.7 (58.1)	1.62 (209)	0.05 (91.3)	2.00 (171)	0.46 (48.8)	54.7 (175)	49.7 (22.9)	57.3 (128)	1.10 (67.2)	0.19 (48.9)
CYP3A4.15	20.9 (123)	32.5 (64.0)	1.27 (164)	0.13 (219)	1.44 (123)	0.32 (33.1)	41.8 (134)	285 (131)	52.8 (118)	0.95 (58.4)	0.25 (63.3)
CYP3A4.16	8.11 (47.9)	36.3 (76.3)	1.11 (147)	0.11 (181)	1.16 (99.7)	0.69 (72.6)	7.10 (22.7)	57.5 (26.4)	26.5 (59.0)	0.29 (17.8)	0.12 (31.5)
CYP3A4.17	N.D.	N.D.	0.08 (11.1)	0.01 (10.3)	0.04 (3.07)	N.D.	0.28 (0.9)	3.1 (1.4)	1.5 (3.3)	N.D.	N.D.

CYP3A4.18	27.2 (161)	45.1 (95.0)	1.55 (200)	0.05 (79.4)	0.55 (46.9)	0.80 (83.9)	19.1 (61.0)	38.3 (17.6)	25.8 (57.5)	0.76 (46.9)	0.12 (31.1)
CYP3A4.19	22.4 (130)	113 (239)	1.68 (222)	0.07 (122)	1.03 (87.9)	0.42 (43.7)	27.4 (87.8)	93.5 (43.0)	43.3 (96.4)	1.02 (62.6)	0.17 (43.1)
488				0.00 (5.5)	N.D.	N.D.	N.D.	8.3 (3.8)	1.3 (2.9)	N.D.	N.D.
Frameshift											
CYP3A4.21								5.3 (2.4)		N.D.	N.D.
CYP3A4.23	35.0 (207)	65.5 (132)	1.69 (220)	0.01 (12.9)	0.47 (39.9)	0.08 (8.6)	4.25 (45.6)	77.9 (35.8)	24.8 (55.2)	0.76 (46.7)	0.11 (27.7)
CYP3A4.24	4.93 (30.3)	N.D.	0.02 (2.67)	0.02 (31.0)	1.10 (94.2)	0.16 (16.5)	22.9 (73.2)	50.3 (23.1)	42.7 (95.1)	1.19 (73.0)	0.23 (59.2)
Pro389Ser										0.30 (18.2)	0.07 (17.8)
Leu475Val										0.46 (28.4)	0.08 (20.1)
CYP3A4.28	17.9 (105)	18.9 (39.6)	0.71 (93.9)	0.03 (47.6)	1.54 (132)	0.52 (55.1)	18.1 (58.0)	218 (100)	41.1 (91.5)	1.06 (65.0)	0.16 (41.5)
CYP3A4.29	24.1 (142)	22.3 (46.7)	1.31 (173)	0.03 (51.2)	1.05 (89.9)	0.40 (41.5)	27.6 (88.5)	689 (317)	29.4 (65.5)	0.54 (33.2)	0.11 (28.4)
CYP3A4.30	N.D.					N.D.	N.D.	N.D.			

CYP3A4.31	33.6 (198)	29.0 (60.9)	1.30 (172)	0.04 (57.0)	1.49 (127)	0.29 (30.3)	26.2 (83.8)	130 (59.7)	27.9 (62.1)	1.47 (90.4)	0.31 (79.4)
CYP3A4.32	30.7 (183)	28.6 (60.0)	1.31 (173)	0.05 (76.4)	0.92 (78.5)	0.16 (16.3)	16.0 (51.2)	164 (75.2)	24.5 (54.6)	0.61 (37.5)	0.22 (54.6)
CYP3A4.33	14.4 (85.2)	46.6 (97.3)	0.88 (117)	0.03 (46.0)	1.00 (85.3)	0.18 (18.5)	16.6 (53.3)	76.2 (35.0)	26.6 (59.2)	0.76 (46.9)	0.06 (14.5)
CYP3A4.34	28.1 (154)	138 (291)	1.17 (155)	0.02 (31.0)	0.50 (42.6)	0.33 (34.6)	17.7 (56.8)	260 (120)	30.8 (68.6)	1.48 (91.0)	0.26 (66.8)

---

N.D. represents not determined.